WHC-SA--1379

DE92 002915

Calculation of the Fast Flux Test Facility Fuel Pin Tests with the WIMS-E and MCNP Codes

K. N. Schwinkendorf
W. D. Wittekind
H. Toffer

Date Published
October 1991

To Be Presented at
1992 Topical Meeting on
Advances In Reactor Physics
Charleston, South Carolina
March 8-11, 1992

Prepared for the U.S. Department of Energy
Assistant Secretary for Nuclear Energy

Westinghouse Hanford Company
P.O. Box 1970
Richland, Washington 99352

Hanford Operations and Engineering Contractor for the
U.S. Department of Energy under Contract DE-AC06-87RL10930

Approved for Public Release

CALCULATION OF THE FAST FLUX TEST FACILITY FUEL PIN TESTS WITH THE WIMS-E AND MCNP CODES

K. N. Schwinkendorf
W. D. Wittekind, H. Toffer
Westinghouse Hanford Company

ABSTRACT

The Fuel Assembly Area (FAA) at the Fast Flux Test Facility site on the Hanford Site at Richland, Washington currently is being prepared to fabricate mixed oxide fuel (U, Pu) for the FFTF. Calculational tools are required to perform criticality safety analyses for various process locations and to establish safe limits for fissile material handling at the FAA. These codes require validation against experimental data appropriate for the compositions that will be handled. Critical array experiments performed by Bierman[1] provide such data for mixed oxide fuel in the range Pu/(U+Pu) = 22 wt%, and with Pu-240 contents equal to 12 wt%. Both the Monte Carlo Neutron Photon (MCNP) and the Winfrith Improved Multigroup Scheme (WIMS-E) computer codes were used to calculate the neutron multiplication factor for explicit models of the various critical arrays. The W-CACTUS module within the WIMS-E code system was used to calculate k_∞ for the explicit array configuration, as well as few-group cross sections that were then used in a three-dimensional diffusion theory code for the calculation of k_{eff} for the finite array.

INTRODUCTION

The Fuel Assembly Area (FAA) at the Fast Flux Test Facility (FFTF) site currently is being prepared to fabricate mixed oxide fuel for the FFTF. Various sources of plutonium are being considered, including the product from N Reactor. Because the Pu-240 content is not yet determined, the criticality analysis requires a parametric treatment of this variable. Calculational tools require validation against experimental critical data. The Bierman critical array experiments[1,2] provide these data for mixed oxide fuel with the ratio Pu/(U+Pu) = 22 wt%. Two computer codes, the WIMS-E modular code system and the MCNP (version 4.2) code, were used to model these experiments.

DESCRIPTION OF EXPERIMENTS

The Bierman[1,2,9,10] experiments consist of mixed-oxide $(U,Pu)O_2$ fuel rods, stainless steel clad, arranged in square arrays, with 15 cm or more of reflection on all sides. Several sets of experiments were performed, including different materials for both moderator and reflector. Various lattice pitches were used in the arrays, resulting in different numbers of fuel rods being required to attain criticality. In the first set of experiments, which were both water moderated and reflected, six different arrays were analyzed. Figures 1 through 6 illustrate these arrays. Two types of fuel pins were used in experiment 003R, with compositions (adjusted for Pu-241 decay) contained in Table 1. The more reactive Type 3.1 pins were used on the periphery, at a larger lattice pitch. All other arrays used only Type 3.2 pins. The stack density of Type 3.1 pins was 9.783 g/cm^3, and 9.830 g/cm^3 for Type 3.2 pins.

DESCRIPTION OF ANALYSIS METHODS AND PROCESS

The British WIMS-E system[3] is a collection of neutronics modules that are used together to perform calculations. Separate modules exist for one-dimensional (1D) integral transport calculations in either cylindrical or slab geometry, with the user's choice of numerical solution techniques. Also included are two-dimensional (2D) transport modules, for either (x,y) or (r,θ) coordinates. Additional modules exist for detailed self-shielded resonance integral calculations in tube-in-tube fuel geometries, collapsing cross sections in space and energy, merging data files, depletion calculations, etc.

The Bierman[1,2] arrays were analyzed by first generating cross sections appropriate for a single fuel pin, then using these cross sections in the 2D transport module W-CACTUS. This single fuel pin was surrounded by moderator to a cylindricized cell boundary, equal in area to the square-array lattice area. The WIMS-E modules W-THES and W-PIP were used to perform these calculations for each fuel type in 69 energy groups. The W-THES module calculates cylindrical collision probabilities according to the Bonalumi method[4]. The W-PIP module calculates the flux solution, which then is used to collapse cross sections for each material to an 18-group set of cross sections. These 18-group data were then employed in the W-CACTUS module.

The W-CACTUS[5] solves the multi-group transport equations in (x,y) geometry using the "method of characteristics," a numerical solution to the differential Boltzmann equation. The user specifies the maximum allowable separation between the 2D "track" mesh. Both azimuthal- and polar-angular integrations are performed numerically, with user-specified angular mesh for the transport approximation. Explicit representation of imbedded cylindrical "inserts" (in this case, fuel pins with cladding) are allowed within the cartesian mesh.

The W-CACTUS flux iteration uses Chebychev polynomial source extrapolation. This accelerates convergence, but numerical instability may occur when there are strong spatial flux gradients. When modeling a repeating unit with relatively weak spatial flux gradients [i.e., a Pressurized Water Reactor (PWR) assembly within a core], the Chebychev routines converge very rapidly, usually after 5 to 10 outer iterations. However, when there are large portions of the problem without fissile material, such as a large reflector, Chebychev extrapolation will become unstable, usually after 10 to 15 iterations. A solution to this problem is to turn off the Chebychev extrapolation after a few iterations.

The Bierman[1,2] critical experiments were modeled with five Chebychev extrapolations. The balance of the flux iteration was performed using nonoverrelaxed "power iteration." This approach removes the Chebychev numerical instability. Unfortunately, long running times result because, in some cases, hundreds of outer iterations were required to converge k_{eff} to within 10^{-5}. Additionally, there are user-defined criteria on volume element-wise flux and boundary angular flux convergence.

The cross-section library used by WIMS-E is the 69-group '1986' WIMS-E library, created by Winfrith[6].

The W-CACTUS is limited by the choice of boundary conditions, either reflective or periodic boundary conditions at the outer periphery, but not zero flux or zero incoming neutron current. It is not possible to model rigorously a neutronically isolated system. However, if the reflector is "thick enough," the distance between arrays is sufficient for effective neutronic isolation to model a single array. Experiment 029 was modeled using the 15.0-cm thickness as shown in Figure 5, but also with 20.4- and 24.0-cm reflector thicknesses. Figure 7 shows that k_{eff} converged to somewhat lower values with thicker reflectors. It was decided that 15.0 cm was sufficient for the purpose of generating cross sections for 3DN, so the rest of the critical arrays were modeled with 15.0-cm reflectors.

After 2D transport convergence, cross sections were collapsed into two groups, for both the fuel and reflector regions. These two-group, two-region cross sections were then input to 3DN, a 3D diffusion theory code used extensively at the Hanford Site[7]. This code allowed for modeling the (x,y) layout with finite axial dimensions. A top and bottom reflector of 15.0 cm also was modeled with 3DN. The k_{eff} produced by 3DN, using two-group cross sections obtained from a 2D transport model of the actual array, were compared to the experimental k_{eff} (which was equal to unity).

The MCNP code[8] uses random numbers to simulate particle transport through three-dimensional (3D) geometries. Statistical estimates then are made on parameters of interest, which may include k_{eff} and flux at certain desired volumes. Nuclear cross sections are obtained from the ENDF/B version V nuclear data library and are treated in MCNP as continuous functions of energy. The advantages of MCNP include the ability to treat highly complicated 3D geometries and the lack of spatial and energy group averaging. Disadvantages include long execution times to obtain reasonable statistical estimates on k_{eff}, especially for large or complicated geometries.

RESULTS

Figures 8 through 12 show W-CACTUS k_{eff} values as a function of iteration for all critical arrays. Table 2 contains the WIMS-E/3DN results. The k_{∞} column refers to the eigenvalue produced by the W-THES module, which performed the initial pincell calculation. The k_{2D} column refers to the value that W-CACTUS converged to, which represents the 2D transport calculation (finite in (x,y) but with no axial leakage correction). The k_{eff} column, produced with 3DN and using two-group cross sections produced by WIMS-E, is the final prediction for the k_{eff} of the critical array.

Accuracy is lost when numerical approximations treat the energy dependence of cross sections by using group-averages. For thermal systems, this approach is usually a very good approximation. However, in harder neutron spectra, the prediction of system reactivity is more sensitive to the treatment of resonance absorption. Fast reactor calculations are performed in many more than two or four groups. The Bierman[1,2] critical array experiments represent a wide range of lattice spacings. As the lattice spacing is reduced, the lattice becomes more under-moderated, requiring additional fuel pins to attain criticality. As a fissile system becomes more under-moderated, the neutron spectrum shifts to higher energies (i.e., the spectrum becomes harder). As a result, more neutron energy groups are required to predict accurately the system reactivity. Experiment 006 represents the largest lattice spacing

analyzed, and the fewest number of pins required for criticality. The W-CACTUS calculations performed for this array (as well as experiments 004 and 001) in 18 energy groups produced two-group cross sections that allowed 3DN to calculate a k_{eff} that was very close to unity (within just a few mk of critical). For the closer-spaced lattices (experiments 029, 005, and 003R) the accuracy began to erode. Experiments 006 and 005 also were evaluated by performing W-CACTUS transport calculations in two and four energy groups. The same two-group cross sections were then extracted from each of these calculations, and fed into 3DN. For experiment 005, both four-group and two-group W-CACTUS calculations produced cross sections for 3DN that resulted in critical predictions much less accurate than the 18-group calculation. This comparison is shown in Figure 13. For experiment 006, the 18-group approach was already accurate; the accuracy penalty in going to either four or two groups was not as severe. This comparison is shown in Figure 14.

Table 2a contains the 3DN results for both experiments 006 and 005, given cross sections that were produced by W-CACTUS using 18, 4, and 2 energy groups for the main transport calculation. Performing transport calculations with W-CACTUS requires a large amount of disk space. Large "scratch files" are created by W-CACTUS while execution proceeds. These files contain detailed geometry tracking information for the problem. When there are many spatial mesh, many energy groups, and a high-order transport calculation is required (azimuthal and polar angles), these parameters will multiply to produce enormous scratch files. The one large scratch file produced by W-CACTUS for array 003R was in excess of 1 GB. It was not practical to increase the number of W-CACTUS energy groups beyond 18 for the larger arrays.

MCNP was used to compare with WIMS-E models of the Bierman[1,2] criticality tests. MCNP was used with reflecting planes above and below the Bierman[1,2] lattice to simulate the WIMS-E k_∞ calculation with 15.0 cm of radial water reflector around the lattice. MCNP was also used with a lattice three feet high and 15.0 cm of axial water reflector as well as the 15.0 cm of radial reflector around the lattice.

These water moderated critical experiments also were computed by MCNP using a more physical representation of the actual geometry, which included explicit representation of upper support structures.

For experiment 006, Figure 15 illustrates the k_{eff} produced by MCNP as a function of neutron generation. The upper and lower curves represent the confidence bounds for $k_{eff} \pm 2\sigma$. Summarizing the comparison between WIMS-E/3DN and MCNP, Table 5 combines the results computed with the two codes.

Similar water-moderated critical experiments, but with concrete reflectors[9], were analyzed by MCNP using the more physical representation geometry. Results are shown in Table 6.

Similar critical experiments were performed[10] using a liquid organic moderator instead of water. These arrays also were computed by MCNP using a physical representation of the actual geometry. Results are shown in Table 7.

CONCLUSIONS

This work illustrates the application of state-of-the-art neutronics codes to evaluation of benchmark critical experiments. Both stochastic and deterministic approaches were used. Both WIMS-E/3DN and MCNP predicted k_{eff}=1 to acceptable accuracy. Execution times for WIMS-E and MCNP were comparable for the calculations performed. However, shortening execution times for MCNP would require simulating fewer neutrons, with the penalty being in the statistical uncertainty in the answer. WIMS-E required long running times because of the nonoverrelaxed nature of the flux iterations. As currently implemented, Chebychev polynomial source extrapolation becomes numerically unstable on some types of problems. Future modifications to W-CACTUS could address these stability problems reducing computing time.

The W-CACTUS, as currently coded, does not have the user-option of specifying boundary conditions consistent with an isolated array. The choices are either reflective or periodic. If a single isolated system is to be modeled, there must be sufficient reflector thickness for the array to be effectively isolated from the rest of the arrays in the "infinite lattice," which reflective boundary conditions imply. In practice, it was found that beyond 15.0 cm, the k_{eff} produced by W-CACTUS did not decrease significantly. All critical arrays were modeled using a 15.0-cm reflector thickness, which, because of symmetry, provides a total distance between arrays in the W-CACTUS model equal to 30.0 cm.

Another source of error that would tend to adjust the WIMS-E/3DN eigenvalue arises because the axial reflector (15.0 cm of water, top and bottom) was modeled as a "pure material." The metal structure (springs inside the cladding, above each fuel pin column, etc.), penetrating the top reflector, was not modeled. The inclusion of these refinements would have resulted in increased neutron streaming through the top reflector, as well as increased neutron absorption in these regions.

REFERENCES

1. Bierman, S. R., "Criticality Experiments with Fast Flux Test Facility Fuel Pins," *Trans. Am. Nucl. Soc., Vol. 62*, November 1990.

2. Bierman, S. R., B. M. Durst, E. D. Clayton, and R. I. Scherpelz, "Critical Experiments with Fast Test Reactor Fuel Pins in Water," *Nuclear Technology, Vol. 44*, June 1979.

3. Gubbins, M. E., M. J. Roth, and C. J. Taubman, *A General Introduction to the Use of the WIMS-E Modular Program*, AEEW-R 1329, Reactor Physics Division, AEE Winfrith, England, June 1982.

4. Roth, M. J., *The Collision Probability Modules of WIMS-E*, Appendix IV, AEEW-R 1920, Reactor Physics Division, AEE Winfrith, England, April 1985.

5. Halsall, M. J., *A User's Guide to the WIMS-E Module W-CACTUS*, AEEW-R 1710, Reactor Physics Division, AEE Winfrith, England, November 1983.

6. Halsall, M. J., and C. J. Taubman, *The '1986' WIMS Nuclear Data Library*, AEEW-R 2133, Reactor Physics Division, AEE Winfrith, England, September 1986.

7. Burnside, R. J., and R. M. Wu, *3DN Computer Code User's Manual*, UNI-M-182, July 1985.

8. Breismeister, J. A., Ed., LA-7396-M, Rev 2, *MCNP - A General Monte Carlo Code for Neutron and Photon Transport*, Version 3A, Los Alamos National Laboratory, New Mexico, September 1986.

9. Bierman, S. R., B. M. Durst, E. D. Clayton, and B. W. Holmes, "Critical Experiments with Concrete-Reflected Fast Test Reactor Fuel Pins in Water," *Nuclear Technology, Vol. 49*, June 1980.

10. Bierman, S. R., G. R. Smolen, and T. Matsumoto, "Experimental Criticality Data Comparing Organic with Water Moderation," *Transactions of the American Nuclear Society, Vol. 54*, June 1987.

Table 1. Isotopic Compositions (wt%) for Bierman Critical Experiments.

Isotope	Type 3.1 Pins Experiment 003R	Type 3.2 Pins Experiment 029	Type 3.2 Pins All other Exps
Pu^{238}	0.0130	0.0111	0.0111
Pu^{239}	21.0641	17.1251	17.1251
Pu^{240}	2.8606	2.3150	2.3150
Pu^{241}	0.3124	0.2493	0.2596
Pu^{242}	0.0526	0.0381	0.0381
Am^{241}	0.0841	0.0980	0.0877
U^{235}	0.4547	0.4853	0.4853
U^{238}	63.5857	67.8638	67.8638
O^{16}	11.5728	11.8143	11.8143

Table 2. The WIMS-E/3DN Calculations of Array Reactivity.

Exp. #	# of Pins	LP (cm)	k_∞ (THES)	k_{2D} (CACTUS)	k_{eff} (3DN)
006	162	1.9050	1.472111	1.002421	1.000681
004	205	1.5342	1.530770	1.016204	0.992811
001	279	1.2588	1.531370	1.024201	0.996414
029	580	0.9677	1.465992	1.043800	1.008973
005	605	0.9525	1.461692	1.043902	1.009545
003R/Type 3.2	972	0.7671	1.389339	---	---
003R/Type 3.1	65	1.5342	1.545231	1.046685	1.014506

Note: There were two pin types in experiment 003R, totaling 1,037.

Table 2a. The 3DN Results Using Different W-CACTUS Cross Sections.

Number of groups	Experiment 006	Experiment 005
18 group W-CACTUS	1.000681	1.009545
4 group W-CACTUS	1.006258	1.037952
2 group W-CACTUS	1.031816	1.053336

Table 3. The MCNP Calculations of Array Reactivity.

Experiment Number	Lattice Spacing (cm)	Number of Pins	Infinite Length	Finite Length
003R	0.7671	1037	1.022760 ± 0.0017	1.000711 ± 0.0015
005	0.9525	605	1.022739 ± 0.0017	1.004087 ± 0.0016
029	0.9677	580	1.023269 ± 0.0017	1.000378 ± 0.0016
001	1.2588	279	1.023606 ± 0.0018	0.997788 ± 0.0016
004	1.5342	205	1.022559 ± 0.0016	1.004184 ± 0.0016
006	1.9050	162	1.024144 ± 0.0015	1.006262 ± 0.0015

Table 4. The MCNP Calculations of Array Reactivity.

Experiment Number	Lattice Spacing (cm)	Lattice Width (pins)	Number of Pins	Physical Representation
003R	0.7671	36	1037	0.994129 ± 0.0016
005	0.9525	28	605	1.003073 ± 0.0017
029	0.9677	28	580	1.002819 ± 0.0017
001	1.2588	18	279	1.004571 ± 0.0018
004	1.5342	18	205	1.004090 ± 0.0016
006	1.9050	14	162	1.007570 ± 0.0016

Table 5. Comparison of WIMS-E/3DN vs. MCNP for Critical Arrays.

Experiment Number	W-CACTUS (2D transport)	3DN (3D diffusion)	MCNP, Infinite Length	MCNP, Finite Length
003R	1.046685	1.014506	1.022760 ± 0.0017	1.000711 ± 0.0015
005	1.043902	1.009545	1.022739 ± 0.0017	1.004087 ± 0.0016
029	1.043800	1.008973	1.023269 ± 0.0017	1.000378 ± 0.0016
001	1.024201	0.996414	1.023606 ± 0.0018	0.997788 ± 0.0016
004	1.016204	0.992811	1.022559 ± 0.0016	1.004184 ± 0.0016
006	1.002421	1.000681	1.024144 ± 0.0015	1.006262 ± 0.0015

Table 6. The MCNP Calculations of Concrete Reflected Critical Experiments.

Experiment Number	Lattice Spacing (cm)	Lattice Width (pins)	Number of Pins	Physical Representation
010	0.953	28	554	1.001748 ± 0.0017
007	1.263	18	260	1.012778 ± 0.0018
012	1.541	18	191	1.010110 ± 0.0017
011	1.906	14	152	1.002032 ± 0.0017

Table 7. The MCNP Calculations of Liquid Organic Moderated Critical Experiments.

Experiment Number	Lattice (cm)	Lattice Width (pins)	Number of Pins	Physical Representation
065	0.761	36	1037	1.001857 ± 0.0017
063	0.968	28	579	1.003641 ± 0.0017
062	1.242	18	279	1.006359 ± 0.0017
061	1.537	18	205	1.006766 ± 0.0019
060	1.935	14	162	1.005103 ± 0.0015

Figure 1. The WIMS-E Model for Critical Experiment 006.

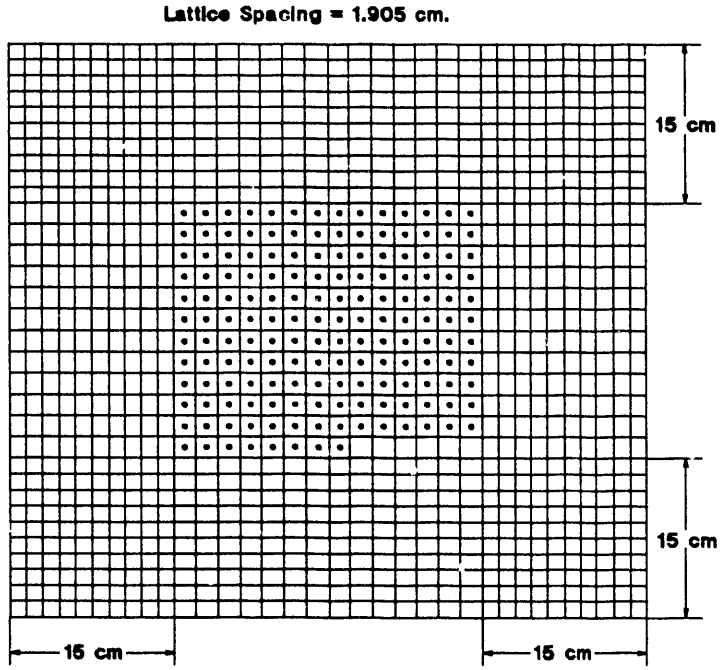

Figure 2. The WIMS-E Model for Critical Experiment 001.

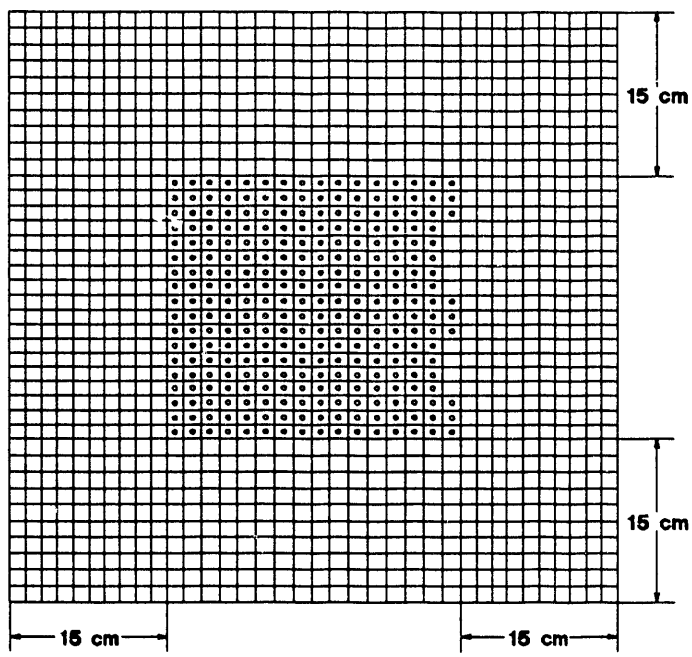

Figure 3. The WIMS-E Model for Critical Experiment 004.

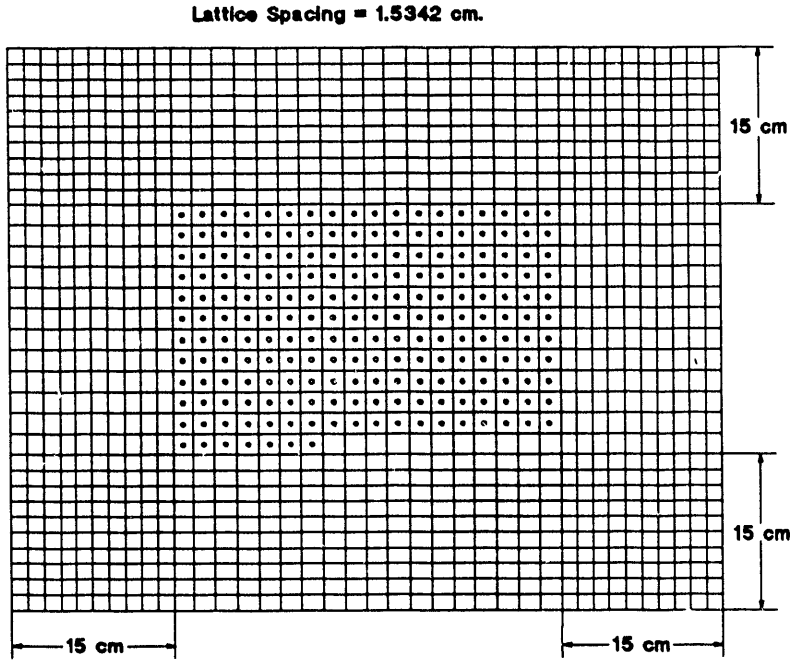

Figure 4. The WIMS-E Model for Critical Experiment 005.

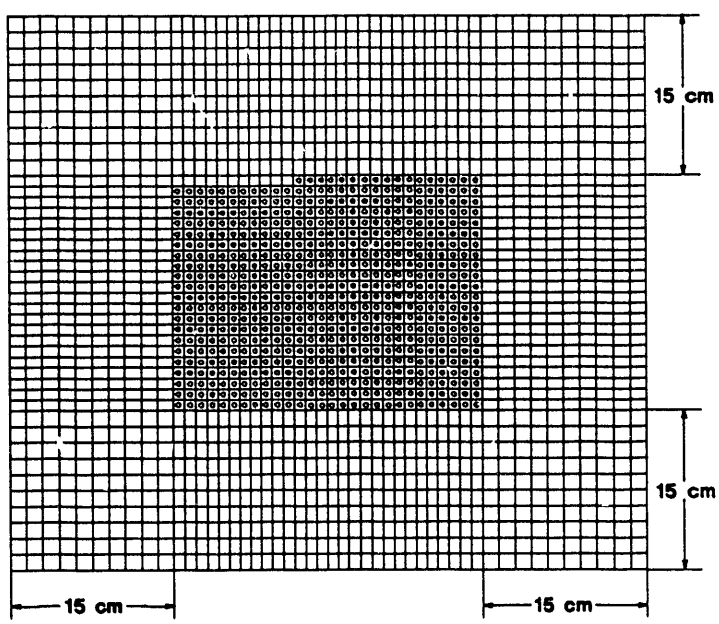

Figure 5. The WIMS-E Model for Critical Experiment 029.

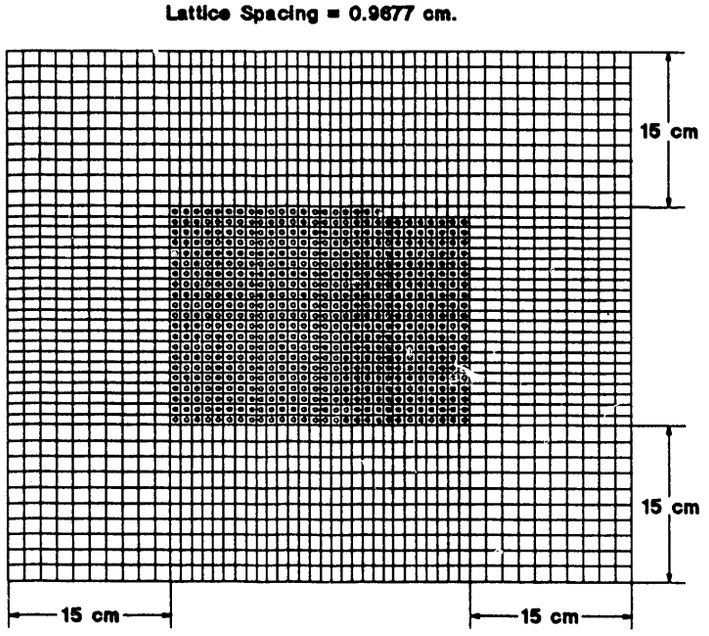

Figure 6. The WIMS-E Model for Critical Experiment 003R.

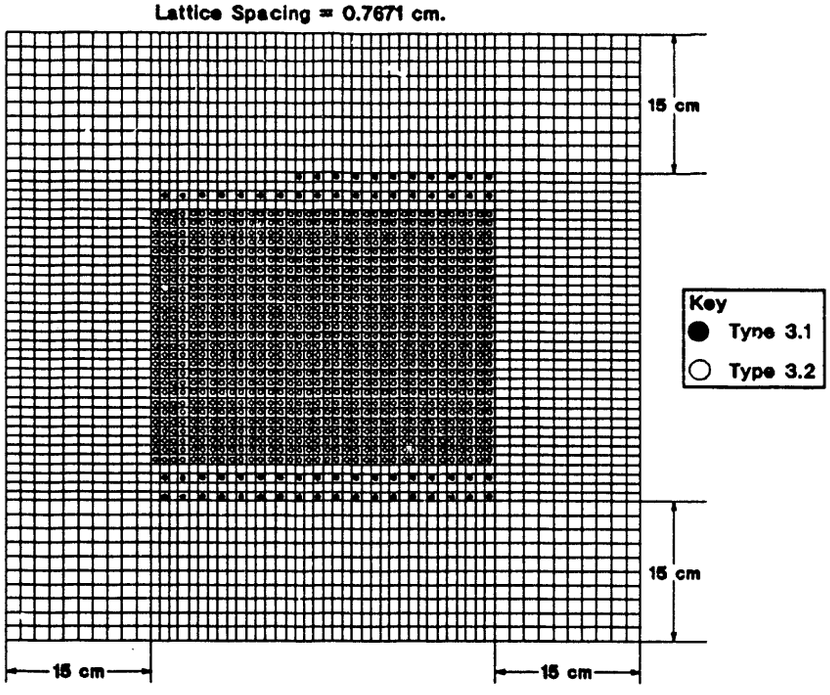

Figure 7. The W-CACTUS k-eff vs. Iteration.
Critical Experiment 029.

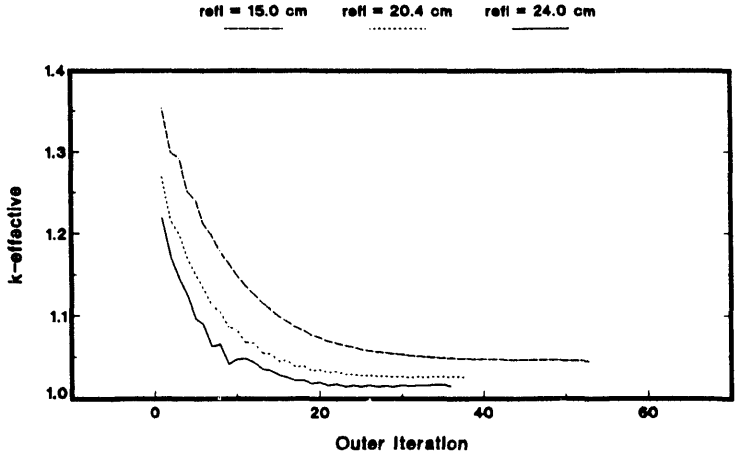

Figure 8. The WIMS-E Convergence Behavior.
Critical Experiment 006.

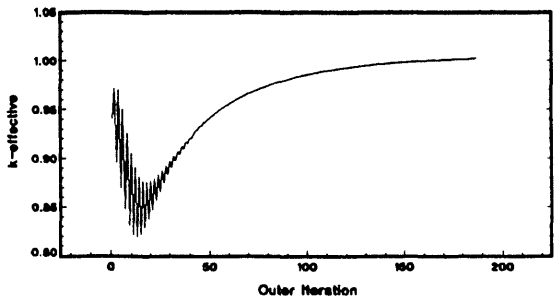

Figure 9. The WIMS-E Convergence Behavior.
Critical Experiment 004.

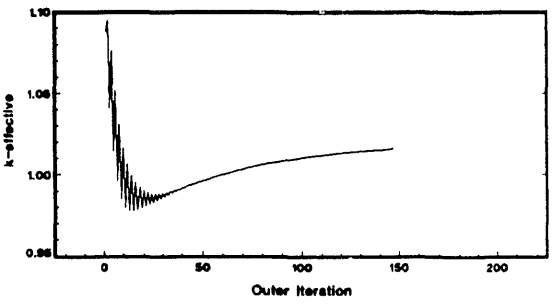

Figure 10. The WIMS-E Convergence Behavior.
Critical Experiment 001.

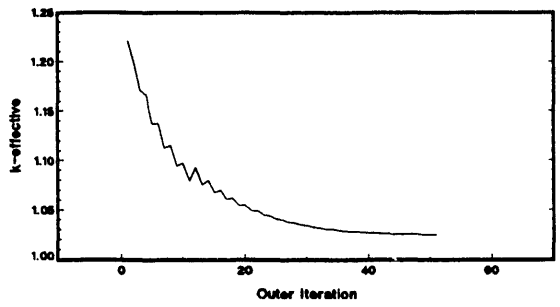

Figure 11. The WIMS-E Convergence Behavior.
Critical Experiment 005.

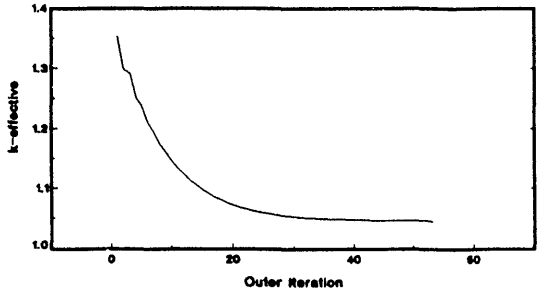

Figure 12. The WIMS-E Convergence Behavior.
Critical Experiment 003R.

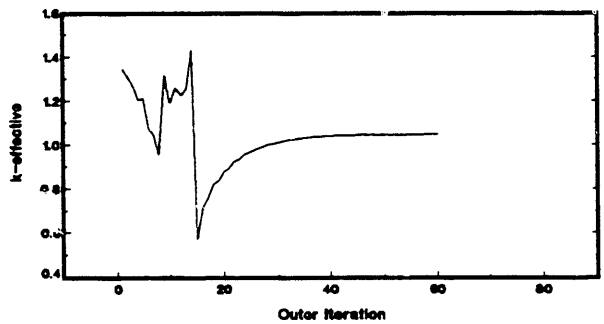

Figure 13. The W-CACTUS k-eff vs. Iteration.
Critical Experiment 005.

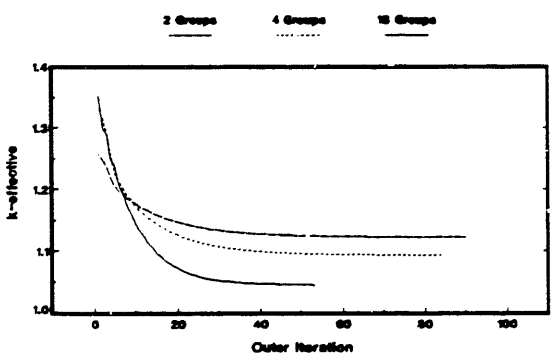

Figure 14. The W-CACTUS k-eff vs. Iteration.
Critical Experiment 006.

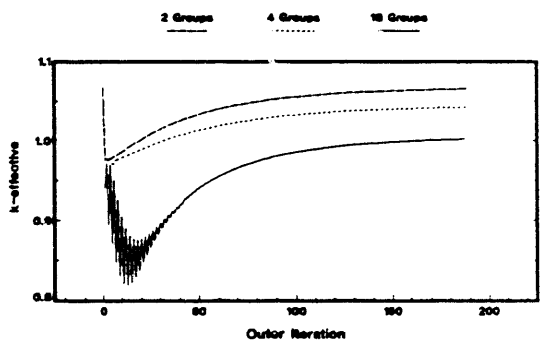

Figure 15. The MCNP k-eff vs. Neutron Generation.
Critical Experiment 006.

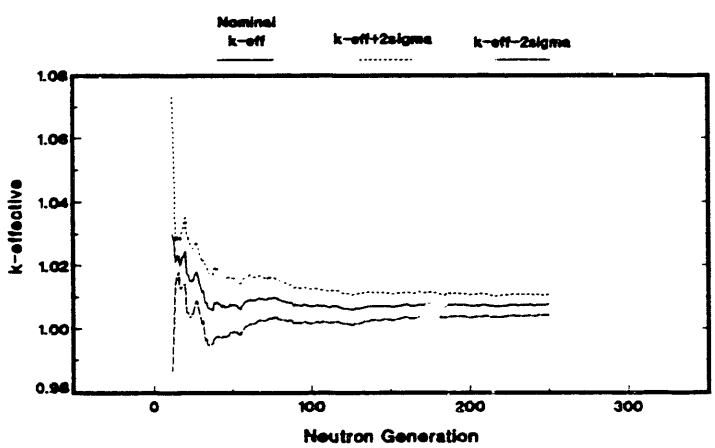

DISTRIBUTION

Number of copies

ONSITE

1 U.S. Department of Energy
Field Office, Richland

R. A. Almquist A6-55

8 Westinghouse Hanford Company

D. L. Crockford H4-17
K. N. Schwinkendorf (2) HO-38
H. Toffer HO-38
W. D. Wittekind HO-38
Publication Services (3)

END

DATE
FILMED
2 10 5 92

I